Sensitivity of sub-critical mode-coupling instabilities in non-conservative rotating continua to stiffness and damping modifications

Oleg N. Kirillov

Dynamics and Vibrations Group, Department of Mechanical Engineering,
Technische Universität Darmstadt, Hochschulstr. 1, 64289 Darmstadt, Germany
Email: kirillov@dyn.tu-darmstadt.de

ABSTRACT:

Mode-coupling instability is a widely accepted mechanism for the onset of friction-induced vibrations in car brakes, wheel sets, paper calendars, to name a few. In the presence of damping, gyroscopic, and non-conservative positional forces the merging of modes is imperfect, that is two modes may come close together in the complex plane without collision and then diverge so that one of the modes becomes unstable. In non-conservative rotating continua that respect axial symmetry this movement of eigenvalues is very sensitive to the variation of parameters of the system. Our study reveals some general rules that govern sub-critical mode-coupling instabilities in non-conservative rotating continua to stiffness and damping modifications and provide useful insight for optimisation of such systems and interpretation of experimental results.

CITATION:

O.N. Kirillov. 2011. Sensitivity of sub-critical mode-coupling instabilities in non-conservative rotating continua to stiffness and damping modifications, *Int. J. Vehicle Structures & Systems*, 3(1), 1-13.

1. Introduction

Mode coupling is generally acknowledged to be one of the most important mechanisms leading to self-excited vibration in relative sliding systems with friction, see e.g. [1-15]. Although both modal analysis and transient analysis of the nonlinear system [16, 17] are the two widely accepted complementary methods in modern treatments of such problems, we will concentrate on the former in this paper.

Frequently, linearisation and discretisation of the models derived for the description of the mode-coupling instability in brakes yields a finite-dimensional circulatory system

$$\ddot{\mathbf{x}} + \mathbf{A}\mathbf{x} = 0 \tag{1}$$

where dot denotes time differentiation and $\mathbf{A}$ is a real non-symmetric matrix that is related to potential and non-conservative positional (or circulatory) forces [2, 3, 11-14].

Circulatory system, as given in Eqn. (1), is (marginally) stable if and only if its eigenvalues are pure imaginary and semi-simple, that is each multiple eigenvalue has a number of linearly-independent eigenvectors equal to its algebraic multiplicity [18]. With the change of parameters the eigenvalues move along the imaginary axis until two of them collide with the origination of the double pure imaginary eigenvalue with the Jordan block that then splits into a pair of complex eigenvalues – one with negative an another with positive real part – that causes flutter instability. This is a basic

mechanism of mode-coupling instability without dissipation [18-21].

The boundary between the domain of marginal stability of a circulatory system and the flutter instability domain possesses singularities that correspond to multiple pure imaginary eigenvalues [18]. For example to a double pure imaginary semi-simple eigenvalue with two linearly-independent eigenvectors corresponds a conical singularity in the space of three parameters which can yield a planar cone in the plane of two parameters [18].

In the presence of dissipation a new term enters the equations of motion.

$$\ddot{\mathbf{x}} + \mathbf{D}\dot{\mathbf{x}} + \mathbf{A}\mathbf{x} = 0 \tag{2}$$

where the real symmetric matrix $\mathbf{D}$ corresponds to the damping forces. In case of full dissipation the matrix $\mathbf{D}$ is positive definite. We note however that negative friction-velocity slope yields an indefinite matrix of damping forces [4,5, 8, 22].

In the presence of damping the mode-coupling scenario of instability is changed. The merging of modes becomes imperfect [3], i.e. two eigenvalues move out the imaginary axis, e.g., to the left part of the complex plane, come closer together, pass in the vicinity of each other and after the closest rendezvous one of the eigenvalues sharply turns to the right and crosses the imaginary axis at some new critical value of parameters [3, 19-21]. The new instability threshold corresponds to a simple pure imaginary eigenvalue in contrast to the undamped case where the critical eigenvalue is pure imaginary and

double. Moreover, in the limit of vanishing dissipation the instability threshold of system, as given in Eqn. (2), generically does not tend to that of the undamped system (1). This phenomenon known as the Ziegler's paradox had been explained by Bottema [23, 24] who found that the stability boundary of a circulatory system with dissipation possesses a singularity known as the Whitney umbrella [15, 24]. Recently, this singular surface separating stability and instability domains was observed for the models of drum and disk brakes in [13] and [15], respectively.

In [13, 15] the critical friction coefficient was plotted as a function of two damping parameters. In case of vanishing damping the vertical axis in the three-dimensional parameter space corresponds to the undamped circulatory system, which is marginally stable when the friction coefficient changes from zero to some instability threshold. On the stability interval all the eigenvalues are pure imaginary. The stability boundary of the damped system has self-intersection along the interval of marginal stability of the undamped system. The angle of the self-intersection becomes smaller when the friction coefficient tends to its undamped critical value, where the angle is zero. This degeneracy corresponds to the Whitney umbrella singularity [15, 23-25]. The existence of the singularity on the stability boundary in the presence of damping explains high sensitivity of the onset of the friction-induced oscillations to small dissipative perturbations as well as the imperfect merging of modes that substitutes the mode-coupling instability in the presence of damping.

Recent studies of self-excited instabilities in brakes, motivated by the problems of squeal noise and wear [10], take into account gyroscopic forces, however small they are for these applications, see for example [5-9, 14, 30]. These studies place the problem of friction-induced instabilities in brakes into the context of classical rotor dynamics where non-conservative forces arising in seals and bearings are known since at least 1920s [31-33].

Typical rotor dynamical applications are related to stability of high-speed machinery such as turbine shafts and wheels, circular saws, disks of computer data storage devices, to name a few [34-41]. In such applications gyroscopic forces are significant and it is natural to consider non-conservative and dissipative forces as a perturbation of a conservative gyroscopic system. A convenient instrument of stability analysis of rotors in the engineering practice is frequency-speed – or Campbell – diagrams that plot frequencies of the rotor vibrations versus rotating speed. For perfect solids of revolution the diagram typically consists of the eigencurves that intersect each other at various speeds. The speed at which one of the eigenfrequencies vanishes is called critical. For high speed applications instabilities at the critical speed and in the supercritical speed range are of major importance [31, 37, 42]. It is known that variation in the mass and stiffness distribution may cause the so-called mass- and stiffness- instabilities for such speeds [37-42]. It is remarkable that these instabilities manifest themselves as instability bubbles [43] of complex eigenvalues that originate due to unfolding of double eigenvalues at some crossings of eigencurves of the Campbell diagram of the non-modified system [30-

42, 44-48]. The mass and stiffness instabilities can easily be identified with the interaction of the so-called waves of positive and negative energy – the instability mechanism that is well-known in hydrodynamics and that is typical for Hamiltonian systems such as conservative gyroscopic ones [42, 43]. Indeed, the Campbell diagram is usually interpreted in terms of forward-, backward- and reflected waves travelling along the circumferential direction of the rotating solid of revolution [37, 49, 50]. Interaction of the reflected and forward travelling waves due to mass and stiffness modification is an example of the destabilising interaction of waves of positive and negative energy in the gyroscopic continuum [42, 43].

We see that flutter can easily be excited in the supercritical range of a rotor due to Hamiltonian perturbations such as mass and stiffness redistribution. This is not the case in the subcritical speed range. Here the doublets in the Campbell diagrams that are sources of the combination resonance [49, 50] in the supercritical range just veer away into avoided crossings [36, 37, 39-42, 44-46]. The instabilities in this speed range are provoked by the non-conservative positional forces and by the indefinite damping [8, 22].

Indeed, fundamental studies of Bottema [23, 24] and Lakhadanov [51] had lead to a discovery of a theorem that states that the gyroscopic system with non-conservative positional forces in the absence of dissipation is generically unstable. This means that in the space of the system's parameters a non-conservative gyroscopic system is unstable almost everywhere and can be marginally stable only on a set of a very low dimension, such as a point in a three-dimensional space. It is not surprising that the theorem is repeatedly confirmed by numerical calculations for many particular models of rotors in frictional contact where non-conservative positional (or circulatory) forces naturally appear [4-8, 11, 12, 14, 37-46]. In practice, rotors in frictional contact can be both stable and unstable at different speeds in the subcritical speed range. The natural stabilizing effect is caused by dissipation. Another possible mechanism of stabilisation in the subcritical range is believed to be related to the stiffness modification of the system.

On the one hand, structural optimisation that breaks the symmetry of the rotor or changes the properties of the brake elements such as brake pads is considered as a practical and cheap passive method of elimination of friction-induced vibrations and therefore its consequences such as squeal and wear [4-6, 29, 52-55]. Optimisation of stability of a translating string or beam as well as of a rotating circular string, ring or disc on an elastic foundation and in the frictional contact is in itself a remarkable new class of non-conservative problems of structural optimisation related to the classical Herrmann-Smith paradox and to the optimal design of columns under conservative and non-conservative loads [54-58].

On the other hand, one can consider the wear as a source of modification of different properties of the brake mechanism such as stiffness distribution, and contact and damping characteristics and may be interested in the sensitivity analysis of the instability onset to such imperfections [10, 27, 28]. For example,

regarding the contact surface topography, by means of experimental analysis some researchers found that the roughness of relative sliding contact surfaces definitely influences the generation of the squeal noise. They found that the contact pressure of a sliding surface and the size of its plateaus have great influence on generating squeal noise [10, 26]. Pads with many small contact plateaus tend to generate stronger squeal noise than pads with relatively large plateaus [10]. All this gives enough motivation to the sensitivity analysis of sub-critical mode-coupling instabilities in non-conservative rotating continua to stiffness and damping modifications.

We note that the variation of stiffness only does not change the type of the system – it remains a non-conservative gyroscopic system even if the frequencies of the stiffness matrix are well-separated, i.e. the spectrum of the matrix does not possess the doublets or multiplets. From this point of view, the problem of optimisation of stability of a gyroscopic non-conservative system by stiffness modification is well-posed only when it takes into account damping.

It is quite natural to look at the marginally stable systems such as conservative gyroscopic or circulatory one and study its stabilization or destabilization by dissipation [8, 9, 13, 19-21, 23, 24, 51, 59-66]. Inside the marginal stability domain the conservative gyroscopic or circulatory system has all its eigenvalues pure imaginary. In the presence of damping this stability domain constitutes a part of the boundary that separates regions of asymptotic stability and instability. Since a non-conservative gyroscopic system is unstable in the absence of dissipation and can be asymptotically stable in the presence of dissipation, an intriguing fundamental question thus arises: What is the set in the space of parameters where all the eigenvalues of the system are pure imaginary? How this set is related to the stability boundary of the damped system (where it is enough that only one complex conjugate pair of eigenvalue be pure imaginary and others have negative real parts)?

The answer to these questions in general is a non-trivial problem that should shed light to the mechanism of mode-coupling subcritical instabilities in rotating systems in frictional contact as well as in many other applications where non-conservative gyroscopic systems with dissipation play a role. In the present paper we give some insight with the use of the perturbation theory developed in [8, 9, 42, 67] that is applied to a general non-conservative gyroscopic system, to a brake disc in frictional contact model and to a rotating shaft model.

2. General perturbation of the doublets of an anisotropic rotor system

Following [4-6, 8, 9, 14, 30, 38, 42, 63-66, 68] we consider the finite-dimensional anisotropic rotor system.

$$\ddot{\mathbf{x}} + (2\Omega\mathbf{G} + \delta\mathbf{D})\dot{\mathbf{x}} + (\mathbf{P} + \Omega^2\mathbf{G}^2 + \kappa\mathbf{K} + \nu\mathbf{N})\mathbf{x} = 0$$
(3)

which is a perturbation of the isotropic one

$$\ddot{\mathbf{x}} + 2\Omega\mathbf{G}\dot{\mathbf{x}} + (\mathbf{P} + \Omega^2\mathbf{G}^2)\mathbf{x} = 0.$$
(4)

where $\mathbf{x} \in R^{2n}$, $\mathbf{P} = \text{diag}(\omega_1^2, \omega_1^2, \omega_2^2, \omega_2^2, \ldots \omega_n^2, \omega_n^2)$

is the stiffness matrix, and $\mathbf{G} = -\mathbf{G}^T$ is the matrix of gyroscopic forces defined as

$$\mathbf{G} = \text{blockdiag}(\mathbf{J}, 2\mathbf{J}, \ldots, n\mathbf{J})$$
(5)

where

$$\mathbf{J} = \begin{pmatrix} 0 & -1 \\ 1 & 0 \end{pmatrix}.$$
(6)

The matrices of non-Hamiltonian perturbation corresponding to velocity-dependent dissipative forces, $\mathbf{D} = \mathbf{D}^T$, and non-conservative positional forces, $\mathbf{N} = -\mathbf{N}^T$, as well as the matrix $\mathbf{K} = \mathbf{K}^T$ of the Hamiltonian perturbation that breaks the rotational symmetry, can depend on the rotational speed Ω. The intensity of the perturbation is controlled by the parameters δ, κ, and ν.

Equations in the form (3) and (4) are among standard models of rotor dynamics that go back at least to the work of Brouwer of 1918 [63, 65] and Jeffcott of 1919 [31] and usually arise from the modal analysis of continuous systems [4-6, 8, 9, 14, 30, 31, 34, 35, 37, 42, 44-48, 68].

At $\Omega = 0$ the eigenvalues $\pm i\omega_s$, $\omega_s > 0$, of the isotropic rotor, as given in Eqn. (4), are double semi-simple with two linearly independent eigenvectors. For example, $\omega_s = s$, where s is a natural number,

corresponds to the natural frequency $f_s = \dfrac{s}{2\pi\rho}\sqrt{\dfrac{P}{\rho}}$ of

a circular string of radius r, circumferential tension P, and mass density ρ per unit length [41, 44-47].

Substituting $\mathbf{x} = \mathbf{u}\exp(\lambda t)$ into Eqn. (4) we arrive at the eigenvalue problem

$$\mathbf{L}_0(\Omega)\mathbf{u} := (\mathbf{I}\lambda^2 + 2\Omega\mathbf{G}\lambda + \mathbf{P} + \Omega^2\mathbf{G}^2)\mathbf{u} = 0.$$ (7)

The eigenvalues of the operator $\mathbf{L}_0$ are found in the explicit form

$$\lambda_s^+ = i\omega_s + is\Omega, \quad \overline{\lambda_s^-} = -i\omega_s + is\Omega,$$

$$\lambda_s^- = i\omega_s - is\Omega, \quad \overline{\lambda_s^+} = -i\omega_s - is\Omega,$$
(8)

where the overbar denotes complex conjugate. The eigenvectors of λ_s^+ and $\overline{\lambda_s^-}$ are

$$\mathbf{u}_1^+ = (-i, 1, 0, 0, \ldots, 0, 0)^T,$$

$$\ldots,$$

$$\mathbf{u}_n^+ = (0, 0, \ldots, 0, 0, -i, 1)^T.$$
(9)

where the imaginary unit holds the $(2s - 1)$ st position in the vector $\mathbf{u}_s^+$. The eigenvectors, corresponding to the eigenvalues λ_s^- and $\overline{\lambda_s^+}$, are simply $\mathbf{u}_s^- = \overline{\mathbf{u}_s^+}$.

For $\Omega > 0$, simple eigenvalues λ_s^+ and λ_s^- correspond to the forward and backward travelling waves, respectively, that propagate in the circumferential

direction of the rotor. At the angular velocity $\Omega_s^{cr} = \omega_s/s$ the frequency of the sth backward travelling wave vanishes to zero, so that the wave remains stationary in the non-rotating frame. We assume further in the text that the sequence of the doublets $i\omega_s$ has the property $\omega_{s+1} - \omega_s \geq \Omega_s^{cr}$, which implies the existence of the minimal critical speed $\Omega_{cr} = \Omega_1^{cr} = \omega_1$. When the speed of rotation exceeds the critical speed, some backward waves, corresponding to the eigenvalues $\overline{\lambda_s^-}$, travel slower than the disc rotation speed and appear to be travelling forward (reflected waves).

Introducing the indices $\alpha, \beta, \varepsilon, \sigma = \pm 1$ we find that the eigenvalue branches $\lambda_s^\varepsilon = i\alpha\omega_s + i\varepsilon s\Omega$ and $\lambda_t^\sigma = i\beta\omega_t + i\sigma t\Omega$ cross each other at $\Omega = \Omega_0$ with the origination of the double eigenvalue $\lambda_0 = i\omega_0$ with two linearly-independent eigenvectors $\mathbf{u}_s^\varepsilon$ and $\mathbf{u}_t^\sigma$, where

$$\Omega_0 = \frac{\alpha\omega_s - \beta\omega_t}{\sigma t - \varepsilon s}, \quad \omega_0 = \frac{\alpha\sigma\omega_s t - \beta\varepsilon\omega_t s}{\sigma t - \varepsilon s}. \quad (10)$$

Let $\mathbf{M}$ be one of the matrices $\mathbf{D}$, $\mathbf{K}$, or $\mathbf{N}$. In the following, we decompose the matrix $\mathbf{M} \in R^{2n \times 2n}$ into n^2 blocks $\mathbf{M}_{st} \in R^{2 \times 2}$, where $s, t = 1, 2, \ldots, n$

$$\mathbf{M}_{st} = \begin{pmatrix} m_{2s-1,2t-1} & m_{2s-1,2t} \\ m_{2s,2t-1} & m_{2s,2t} \end{pmatrix}. \quad (11)$$

Note that $\mathbf{D}_{st} = \mathbf{D}_{ts}^T$, $\mathbf{K}_{st} = \mathbf{K}_{ts}^T$, and $\mathbf{N}_{st} = -\mathbf{N}_{ts}^T$.

We consider a general perturbation of the matrix operator of the isotropic rotor $\mathbf{L}_0(\Omega) + \Delta\mathbf{L}(\Omega)$. The size of the perturbation

$$\Delta\mathbf{L}(\Omega) = \delta\lambda\mathbf{D} + \kappa\mathbf{K} + \nu\mathbf{N} \sim \eta \quad (12)$$

is small, where $\eta = \|\Delta\mathbf{L}(\Omega_0)\|$ is the Frobenius norm of the perturbation at $\Omega = \Omega_0$. For small $\Delta\Omega = |\Omega - \Omega_0|$ and η the increment to the doublet $\lambda_0 = i\omega_0$ with the eigenvectors $\mathbf{u}_s^\varepsilon$ and $\mathbf{u}_t^\sigma$, is given by the formula $\det(\mathbf{R} + (\lambda - \lambda_0)\mathbf{Q}) = 0$, where the entries of the 2×2 matrices Q and R are [8, 9, 42, 67]

$$Q_{st}^{\varepsilon\sigma} = 2i\omega_0(\overline{\mathbf{u}}_s^\varepsilon)^T\mathbf{u}_t^\sigma + 2\Omega_0(\overline{\mathbf{u}}_s^\varepsilon)^T\mathbf{G}\mathbf{u}_t^\sigma,$$

$$R_{st}^{\varepsilon\sigma} = (2i\omega_0(\overline{\mathbf{u}}_s^\varepsilon)^T\mathbf{G}\mathbf{u}_t^\sigma + 2\Omega_0(\overline{\mathbf{u}}_s^\varepsilon)^T\mathbf{G}^2\mathbf{u}_t^\sigma)(\Omega - \Omega_0)$$

$$+ i\omega_0(\overline{\mathbf{u}}_s^\varepsilon)^T\mathbf{D}\mathbf{u}_t^\sigma\delta + (\overline{\mathbf{u}}_s^\varepsilon)^T\mathbf{K}\mathbf{u}_t^\sigma\kappa + (\overline{\mathbf{u}}_s^\varepsilon)^T\mathbf{N}\mathbf{u}_t^\sigma\nu. \quad (13)$$

Calculating the coefficients, as given in Eqn. (13), with the eigenvectors, as given in Eqn. (9), we find the real

and imaginary parts of the sensitivity of the doublet $\lambda_0 = i\omega_0$ at the crossing (10),

$$\mathrm{Re}\,\lambda = -\frac{1}{8}\left(\frac{\mathrm{Im}\,A_1}{\alpha\omega_s} + \frac{\mathrm{Im}\,B_1}{\beta\omega_t}\right) \pm \sqrt{\frac{|c| - \mathrm{Re}\,c}{2}}, \quad (14)$$

$$\mathrm{Im}\,\lambda = \omega_0 + \frac{\Delta\Omega}{2}(s\varepsilon + t\sigma)$$

$$+ \frac{\kappa}{8}\left(\frac{\mathrm{tr}\mathbf{K}_{ss}}{\alpha\omega_s} + \frac{\mathrm{tr}\mathbf{K}_{tt}}{\beta\omega_t}\right) \pm \sqrt{\frac{|c| + \mathrm{Re}\,c}{2}}, \quad (15)$$

where $c = \mathrm{Re}\,c + i\,\mathrm{Im}\,c$ with

$$\mathrm{Im}\,c = \frac{\alpha\omega_t\,\mathrm{Im}\,A_1 - \beta\omega_s\,\mathrm{Im}\,B_1}{8\omega_s\omega_t}(s\varepsilon - t\sigma)\Delta\Omega$$

$$+ \kappa\frac{(\alpha\omega_s\mathrm{tr}\mathbf{K}_{tt} - \beta\omega_t\mathrm{tr}\mathbf{K}_{ss})(\alpha\omega_s\,\mathrm{Im}\,B_1 - \beta\omega_t\,\mathrm{Im}\,A_1)}{32\omega_s^2\omega_t^2}$$

$$- \alpha\beta\kappa\frac{\mathrm{Re}\,A_2\mathrm{tr}\mathbf{K}_{st}\mathbf{J}_{\varepsilon\sigma} - \mathrm{Re}\,B_2\mathrm{tr}\mathbf{K}_{st}\mathbf{I}_{\varepsilon\sigma}}{8\omega_s\omega_t}, \quad (16)$$

$$\mathrm{Re}\,c = \left(\frac{t\sigma - s\varepsilon}{2}\Delta\Omega + \kappa\frac{\beta\omega_s\mathrm{tr}\mathbf{K}_{tt} - \alpha\omega_t\mathrm{tr}\mathbf{K}_{ss}}{8\omega_s\omega_t}\right)^2$$

$$- \frac{(\alpha\omega_s\,\mathrm{Im}\,B_1 - \beta\omega_t\,\mathrm{Im}\,A_1)^2 + 4\alpha\beta\omega_s\omega_t((\mathrm{Re}\,A_2)^2 + (\mathrm{Re}\,B_2)^2)}{64\omega_s^2\omega_t^2}$$

$$+ \alpha\beta\frac{(\mathrm{tr}\mathbf{K}_{st}\mathbf{J}_{\varepsilon\sigma})^2 + (\mathrm{tr}\mathbf{K}_{st}\mathbf{I}_{\varepsilon\sigma})^2}{16\omega_s\omega_t}\kappa^2. \quad (17)$$

The coefficients A_1, A_2 and B_1, B_2 depend only on those entries of the matrices $\mathbf{D}$, $\mathbf{K}$, and $\mathbf{N}$ that belong to the four 2×2 blocks (11) with the indices s and t

$$A_1 = \delta\lambda_0\mathrm{tr}\mathbf{D}_{ss} + \kappa\mathrm{tr}\mathbf{K}_{ss} + \varepsilon 2i\nu n_{2s-1,2s},$$

$$B_1 = \delta\lambda_0\mathrm{tr}\mathbf{D}_{tt} + \kappa\mathrm{tr}\mathbf{K}_{tt} + \sigma 2i\nu n_{2t-1,2t},$$

$$A_2 = \sigma\nu\mathrm{tr}\mathbf{N}_{st}\mathbf{I}_{\varepsilon\sigma} + i(\delta\lambda_0\mathrm{tr}\mathbf{D}_{st}\mathbf{J}_{\varepsilon\sigma} + \kappa\mathrm{tr}\mathbf{K}_{st}\mathbf{J}_{\varepsilon\sigma}),$$

$$B_2 = \sigma\nu\mathrm{tr}\mathbf{N}_{st}\mathbf{J}_{\varepsilon\sigma} - i(\delta\lambda_0\mathrm{tr}\mathbf{D}_{st}\mathbf{I}_{\varepsilon\sigma} + \kappa\mathrm{tr}\mathbf{K}_{st}\mathbf{I}_{\varepsilon\sigma}),$$
$$\quad (18)$$

where

$$\mathbf{I}_{\varepsilon\sigma} = \begin{pmatrix} \varepsilon & 0 \\ 0 & \sigma \end{pmatrix}, \quad \mathbf{J}_{\varepsilon\sigma} = \begin{pmatrix} 0 & -\sigma \\ \varepsilon & 0 \end{pmatrix}. \quad (19)$$

Many important low-dimensional models of rotor dynamics are described by the Eqns. (3) and (4) with $n = 1$ [4-6, 31-33, 59, 60, 63-66], see also [7] for an overview of the minimal models for brake squeal and [69-72] for the discussion on model reduction in the problems of non-conservative stability. In this case $\mathbf{N} = \mathbf{J}$ and the only subcritical crossings of the eigencurves (10) happen at $\Omega_0 = 0$ and correspond to $s = t$, $\varepsilon = -\delta = 1$, and $\alpha = \beta = 1$. With these coefficients, the Eqns. (14), (15) and (16), (17) are simplified to

$$\operatorname{Re}\lambda = -\frac{\mu_1+\mu_2}{4}\delta \pm \sqrt{\frac{|c|+\operatorname{Re}c}{2}}, \qquad (20)$$

$$\operatorname{Im}\lambda = \omega_1 + \frac{\rho_1+\rho_2}{4\omega_1}\kappa \pm \sqrt{\frac{|c|-\operatorname{Re}c}{2}}, \qquad (21)$$

$$\operatorname{Re}c = \left(\frac{\mu_1-\mu_2}{4}\right)^2\delta^2 - \left(\frac{\rho_1-\rho_2}{4\omega_1}\right)^2\kappa^2 - \Omega^2 + \frac{v^2}{4\omega_1^2}, \quad (22)$$

$$\operatorname{Im}c = \frac{\Omega v}{\omega_1} - \delta\kappa\frac{2\operatorname{tr}\mathbf{K}\mathbf{D} - \operatorname{tr}\mathbf{K}\operatorname{tr}\mathbf{D}}{8\omega_1}, \qquad (23)$$

where $\mu_{1,2}$ and $\rho_{1,2}$ are the eigenvalues of the 2×2 matrices $\mathbf{D}$ and $\mathbf{K}$, respectively. From the condition $\operatorname{Re}\lambda = 0$, we find the approximation to the boundary of asymptotic stability domain

$$\left(\frac{\mu_1+\mu_2}{4}\right)^2\delta^2 - \frac{\operatorname{Re}c}{2} = \frac{|c|}{2}. \qquad (24)$$

In the absence of gyroscopic and dissipative terms the expression (24) simplifies to

$$\left(\frac{\rho_1-\rho_2}{2}\right)^2\kappa^2 - v^2 = 0. \qquad (25)$$

In the (κ,v) - plane, Eqn. (25) defines two lines intersecting at the origin. The lines separate the flutter instability domain that contains the v-axis (in accordance with the Merkin theorem [59, 60]) and the domain of marginal stability. The flutter domain thus has a form of the planar cone with the apex corresponding to the double semi-simple pure imaginary eigenvalue [18]. In the following we will see how this conical singularity manifests itself in the modelling the disc brakes and rotating shafts.

3. Example 1. A one-doublet mode model of a disc in distributed frictional contact

In [4] Kang, Krousgrill and Sadeghi investigated the dynamic instability due to circumferential friction between a stationary thin annular plate and two fixed annular sector contact interfaces under steady-sliding conditions. The effects of rotation and damping were neglected in their model. By linearization of the governing PDEs and with the use of the truncated modal expansion, the governing equations were obtained in [4] in the form of the linear circulatory system that follows from the Eqn. (3) when $\Omega = 0$ and $\delta = 0$.

For the prediction of squeal a single doublet mode pair model was introduced in [4] with the following matrices of potential forces $\mathbf{P}$, $\mathbf{K}$ and the matrix of circulatory forces $\mathbf{N}$

$$\mathbf{P} = \begin{pmatrix} \omega_{2n}^2 + 0.5k_c\tilde{R}_n^z\theta_c & 0 \\ 0 & \omega_{2n}^2 + 0.5k_c\tilde{R}_n^z\theta_c \end{pmatrix}, \quad (26)$$

$$\kappa\mathbf{K} = \frac{k_c\sin(n\theta_c)}{2n}\begin{pmatrix} \tilde{R}_n^z & \mu n\tilde{R}_n^\theta \\ \mu n\tilde{R}_n^\theta & -\tilde{R}_n^z \end{pmatrix}$$
$$-\begin{pmatrix} \omega_{2n}^2 - \omega_{2n-1}^2 & 0 \\ 0 & 0 \end{pmatrix}, \qquad (27)$$

$$\mathbf{N} = \mathbf{J} = \begin{pmatrix} 0 & -1 \\ 1 & 0 \end{pmatrix}, \quad v = \frac{\mu k_c n\tilde{R}_n^\theta\theta_c}{2}. \qquad (28)$$

In the Eqns. (26)-(28), n is the number of nodal diameters on a vibrating annular plate and is referred to as the mode number. The two neighbouring circular natural frequencies of the stationary disc are denoted as ω_{2n} and ω_{2n-1}. The friction coefficient μ is assumed to be uniformly constant over the contact area of the disc with the contact span angle θ_c. The stiffness of the contact is also uniformly constant and equal k_c. The coefficients $\tilde{R}_n^\theta$ and $\tilde{R}_n^z$ are integrals involving the squared radial functions of order n in the modal expansion for the transverse displacement of the disc [4]. The matrices (27) and (28) are perturbations of the potential system with the matrix (26) for small values of μ and in the vicinity of those values of the contact span angle θ_c that satisfy the equation $\sin(n\theta_c) = 0$.

Calculating the eigenvalues ρ_1 and ρ_2 of the symmetric matrix $\mathbf{K}$ defined by the Eqn. (27) we find

$$\rho_{1,2} = -\frac{\omega_{2n}^2 - \omega_{2n-1}^2}{2\kappa} \pm$$
$$\frac{\sqrt{\left((\omega_{2n}^2 - \omega_{2n-1}^2)n - k_c\tilde{R}_n^z\sin(n\theta_c)\right)^2 + \mu^2k_c^2\tilde{R}_n^\theta{}^2\theta_c^2\sin^2(n\theta_c)n^2}}{2n\kappa}$$
$$(29)$$

Taking their difference, substituting it into Eqn.(25) and taking into account the expression for the parameter v that follows from the Eqn. (28), we find the approximation of the boundary between the domains of marginal stability and flutter

$$\mu^2 = \frac{\left(\omega_{2n}^2 - \omega_{2n-1}^2 - k_c\tilde{R}_n^z\dfrac{\sin(n\theta_c)}{n}\right)^2}{k_c^2(\tilde{R}_n^\theta)^2(n^2\theta_c^2 - \sin^2(n\theta_c))}. \qquad (30)$$

Remarkably, the expression (30) following from the formulas of the perturbation theory of the previous section reproduces the exact solution given in the work [4]. When the frequency separation is zero, i.e. $\omega_{2n}^2 = \omega_{2n-1}^2$, the Eqn. (30) simplifies to

$$\mu = \pm\frac{\tilde{R}_n^z}{\tilde{R}_n^\theta}\frac{\sin(n\theta_c)}{n\sqrt{n^2\theta_c^2 - \sin^2(n\theta_c)}}. \qquad (31)$$

Taking for simplicity $\tilde{R}_n^z = \tilde{R}_n^\theta$ we plot the stability boundary (31) in the (θ_c,μ)-plane for $n = 1$ and $n = 4$, see Fig. 1. For small values of the friction

coefficient μ instability domain has the form of two-dimensional conical tongues with their apexes at $\mu = 0$ corresponding to the double semi-simple roots of the matrix polynomial $\mathbf{I}\lambda^2 + \mathbf{P}$

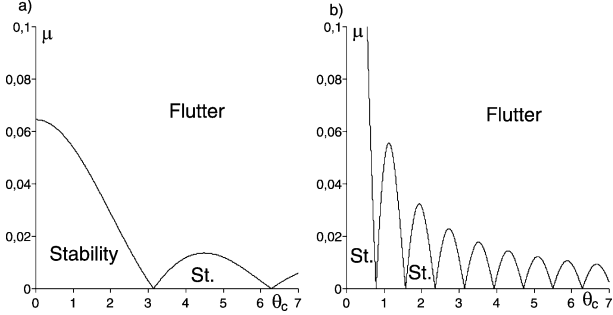$$\lambda = \omega_{2n}^2 + 0.5k_c\tilde{R}_n^z\theta_c. \tag{32}$$

Fig. 1: Domains of marginal stability and flutter for the disc in the case of non-separated frequencies; (a) $n = 1$, (b) $n = 4$

The conical form of the flutter domain of a circulatory system in the vicinity of a point in the parameter space corresponding to the double semi-simple eigenvalue is well-known [18]. In [18] full classification of generic singularities of the stability boundary of a circulatory system was given and approximations to the boundary near the singularities were derived with the use of the perturbation theory of multiple eigenvalues. In particular, the conical singularity of the stability boundary corresponding to the crossing of the eigencurves was analysed in detail.

The shape of the instability tongues illustrates the general theorem by Merkin that states that the potential system with equal frequencies is always destabilized by non-conservative positional forces [59, 60]. Indeed at the singular points the vertical direction leads to the flutter domain as is seen in Fig. 1. Nevertheless detuning the frequencies of the degenerate potential system can stabilize the system for relatively small values of the circulatory forces. We note that Fig. 1 qualitatively agrees with the plots of the work [4]. For the quantitative agreement one needs to take the corresponding values of the ratio $\tilde{R}_n^z / \tilde{R}_n^\theta$.

4. Example 2. The mechanism of subcritical flutter instability for a rotating shaft

Another example of a rotor dynamics system described by Eqns. (3) is a two-degrees-of-freedom model of a rotating shaft [64], see Fig. 2. In [64] the shaft is modelled as the mass m which is attached by two springs with the stiffness coefficients k_1 and $k_2 = k_1 + \kappa$ and two dampers with the coefficients μ_1 and μ_2 to a coordinate system rotating at constant angular velocity Ω, Fig. 2. A non-conservative positional force βr acts on the mass. Such a force on the shaft in the bearings may arise in a rotating fluid or in an electromagnetic field [64].
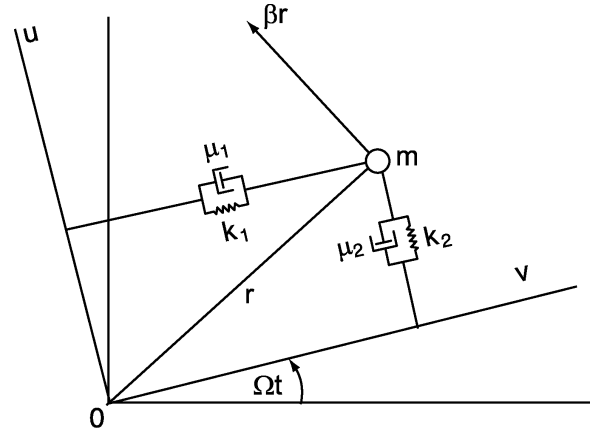

Fig. 2: A model of the rotating shaft by Shieh and Masur [64]

With u and v representing the displacements in the direction of the two rotating coordinate axes, respectively, the system [64] is governed by

$$m\ddot{u} + \mu_1\dot{u} - 2m\Omega\dot{v} + (k_1 - m\Omega^2)u + \beta v = 0,$$

$$m\ddot{v} + \mu_2\dot{v} + 2m\Omega\dot{u} + (k_2 - m\Omega^2)v - \beta u = 0, \tag{33}$$

where dot means time differentiation. Dividing both Eqns. (33) by m, we find that this is a system of type (3) with the matrices

$$\delta\mathbf{D} = \begin{pmatrix} \mu_1 m^{-1} & 0 \\ 0 & \mu_2 m^{-1} \end{pmatrix}, \quad \mathbf{P} = \begin{pmatrix} k_1 m^{-1} & 0 \\ 0 & k_1 m^{-1} \end{pmatrix},$$

$$k\mathbf{K} = \begin{pmatrix} 0 & 0 \\ 0 & \kappa m^{-1} \end{pmatrix}, \quad \nu\mathbf{N} = \begin{pmatrix} 0 & \beta m^{-1} \\ -\beta m^{-1} & 0 \end{pmatrix}. \tag{34}$$

Separating time with the substitution $u = u_0 e^{\lambda t}$, $v = v_0 e^{\lambda t}$ yields the characteristic polynomial

$$p(\lambda) = \lambda^4 + \frac{\mu_1 + \mu_2}{m}\lambda^3 + \left(\frac{\mu_1\mu_2}{m^2} + \frac{k_1 + k_2}{m} + 2\Omega^2\right)\lambda^2$$

$$+ \left(\frac{k_1\mu_2 + \mu_1 k_2}{m^2} - \frac{4\Omega\beta}{m} - \frac{\mu_1 + \mu_2}{m}\Omega^2\right)\lambda$$

$$- \Omega^4 + \Omega^2\frac{k_2 - k_1}{m} + \frac{k_1 k_2 + \beta^2}{m^2}. \tag{35}$$

It is straightforward to see that the polynomial (35) becomes biquadratic in case when the following conditions are fulfilled

$$\mu_1 + \mu_2 = 0, \quad \kappa = \frac{4\Omega\beta m}{\mu_1}. \tag{36}$$

Moreover, all the roots of the polynomial (35) under restraints (36) and sufficiently small perturbations are pure imaginary if, in addition

$$|\mu_1| \le 2|\Omega|m. \tag{37}$$

The equality in (37) corresponds to the double pure imaginary eigenvalues λ with the Jordan block

$$\lambda = \pm\sqrt{\frac{k_1}{m} \pm \frac{\beta}{m} - \Omega^2}. \tag{38}$$

Therefore, in the space of the shaft parameters there exists a non-trivial set given by expressions (36), (37) where all the eigenvalues of the system are pure imaginary (marginal stability) in the presence of dissipative and non-conservative forces. To study the connection of this set to the domains of instability and asymptotic stability in the parameter space, it is more convenient to use the perturbation formulas of the previous section than to analyse directly the characteristic polynomial (35). Indeed, in the absence of perturbations, i.e. when $\kappa = 0$, $\mu_1 = \mu_2 = 0$, and $\beta = 0$, the eigenvalues of the shaft are pure imaginary

$$\lambda(\Omega) = \pm i \sqrt{\frac{k_1}{m}} \pm i\Omega . \qquad (39)$$

The eigencurves (39) cross at $\Omega = 0$ and at $\Omega_{cr} = \pm \sqrt{\frac{k_1}{m}}$. We are interested in the instabilities that develop at rotation speeds $|\Omega| < |\Omega_{cr}|$, i.e., subcritical instabilities [37]. Thus, we have to look at the unfolding of the doublet $\lambda = i\sqrt{k_1/m}$ at $\Omega = 0$.

Substituting the matrices (34) into Eqns. (20)-(23) we find approximations to the real and imaginary parts of the perturbed double eigenvalues.

$$\text{Re}\,\lambda = -\frac{\mu_1 + \mu_2}{4m} \pm \sqrt{\frac{|c| + \sqrt{\text{Re}\,c}}{2}}, \qquad (40)$$

$$\text{Im}\,\lambda = \sqrt{\frac{k_1}{m}} + \frac{\kappa}{4\sqrt{k_1 m}} \pm \sqrt{\frac{|c| - \text{Re}\,c}{2}}, \qquad (41)$$

$$\text{Re}\,c = \left(\frac{\mu_1 - \mu_2}{4m}\right)^2 - \frac{\kappa^2 - 4\beta^2}{16mk_1} - \Omega^2, \qquad (42)$$

$$\text{Im}\,c = -\frac{\Omega\beta}{\sqrt{k_1 m}} - \frac{\kappa(\mu_2 - \mu_1)}{8m\sqrt{k_1 m}}. \qquad (43)$$

From the condition $\text{Re}\,\lambda = 0$ the approximation to the stability boundary immediately follows

$$\frac{(\mu_1 + \mu_2)^2 + 4\mu_1\mu_2}{16m^2} + \frac{\kappa^2 - 4\beta^2}{16mk_1} + \Omega^2 = |c|, \quad (44)$$

$$\mu_1 + \mu_2 > 0. \qquad (45)$$

It is easy to see that in the absence of gyroscopic and dissipative forces when $\mu_1 = \mu_2 = 0$ and $\Omega = 0$ the stability boundary of the circulatory system is given by the expression

$$\kappa^2 = 4\beta^2. \qquad (46)$$

In the (κ, β)-plane the flutter instability is inside the cone given by the inequality $\kappa^2 < 4\beta^2$. Stability domain is given by the opposite inequality $\kappa^2 > 4\beta^2$, Fig. 3. Consequently, when the stiffness detuning

$\kappa = 0$, the potential system with the coincident frequencies (or stiffness coefficients $k_1 = k_2$) is always destabilized by non-conservative positional forces. This is the statement of the Merkin theorem [59, 60]. The conical singularity is one of the generic singularities of the stability boundary of circulatory systems whose full classification and analysis was given in [18]. However, detuning of the stiffness matrix $\kappa \neq 0$ increases the instability threshold for the non-conservative positional force, Fig. 3. Note that the conical singularities of the flutter domain in the (κ, β)-plane are quite typical in the modelling of brake squeal and otpimization of brake elements (such as brake pads), see for instance [4].
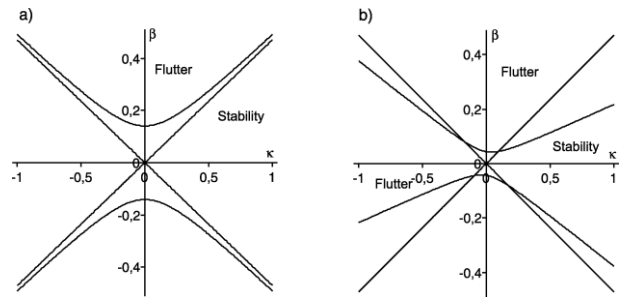

Fig. 3: Approximation to the stability domain in the (κ, β)-plane for $m = 1$, $k_1 = 1$ in the absence of dissipative and gyroscopic forces (straight lines, marginal stability) and (hyperbolic curves, asymptotic stability); (a) $\Omega = 0$, $\mu_1 = 0.1$, $\mu_1 = 0.2$, (b) $\Omega = 0.3$, $\mu_1 = 0.03$, $\mu_1 = 0.06$

In the literature on brake squeal there is a tendency to take into account all possible forces [5, 6]. We look now what happens with the stability boundary in the (κ, β)-plane when damping and gyroscopic forces are added. In the absence of gyroscopic forces ($\Omega = 0$) damping increases the instability threshold as shown in Fig. 3(a). The approximation to the boundary between the flutter and stability domains is given now by hyperbolic curve (44) with the asymptotes (46), Fig. 3(a). Stability domain is between the branches of the hyperbola. When both gyroscopic and damping forces are acting, the instability threshold is lower, Fig. 3(b). The boundary between the stability and flutter domain is approximated by the hyperbolic curve (44) with the asymptotes that differ from the lines (46), Fig. 3(b). Again, stability domain is between the branches of the hyperbola.

To uncover the hidden reasons for the non-trivial transformation of the stability boundary in the presence of non-conservative positional, gyroscopic and dissipative forces, further in the text we will study stability boundary (44), (45) in the (μ_1, μ_2, κ) - space. In the simplest case when $\Omega = 0$ and $\beta = 0$ stability domain is bounded by the inequalities $\mu_1 > 0$ and $\mu_2 > 0$. That is, in the (μ_1, μ_2, κ)- space the stability boundary is a dihedral angle as is seen in Fig. 4(a). Damping does not change the stability domain of the potential system with positive definite matrix **P** [62].

The shape of the stability domain in (μ_1, μ_2) - plane is invariant with respect to the changes in the spectral gap of **P** that is controlled by the parameter κ.

Adding the circulatory forces ($\beta \neq 0, \Omega = 0$) leads to significant qualitative changes in the stability domain and its boundary, Fig. 4(b). It turns out that as soon as a tiny bit amount of non-conservative positional forces is added, the edge of the stability domain along the κ - axis breaks up into two portions, Fig. 4(b). As a result, in the vicinity of the origin stability boundary moves out from the vertical axis opening a round instability window. The stability boundary near the window is smooth almost everywhere and saddle-like, Fig. 4(b). At the points

$$(0, 0, \pm 2\beta), \qquad (47)$$

shown in Fig. 4(b) by the open circles the stability boundary has a singularity Whitney umbrella that corresponds to pure imaginary double eigenvalue (38) with the Jordan block [15, 19-21, 23-25].
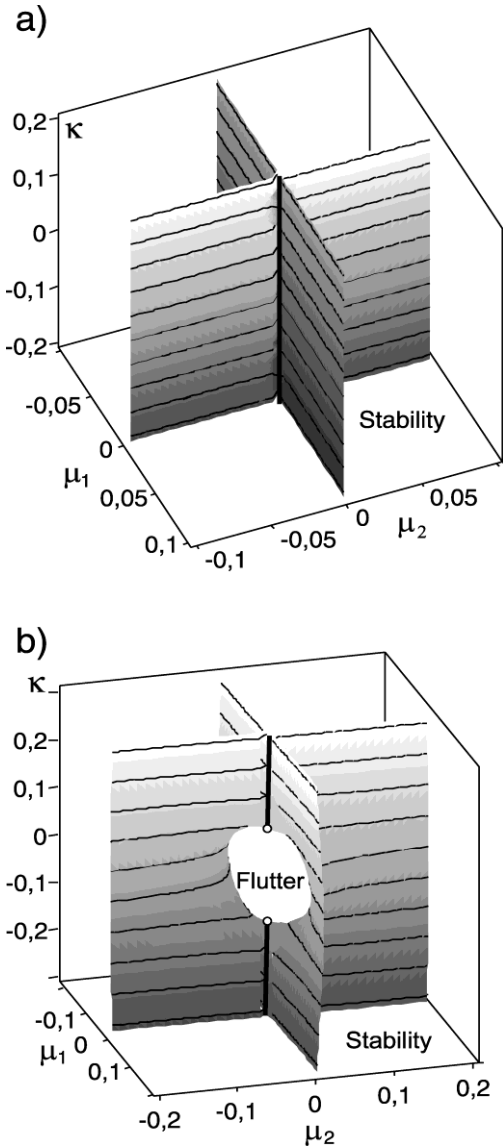
a)

b)

Fig. 4: Approximation to the asymptotic stability domain in the (μ_1, μ_2, κ) **-space for** $m = 1$, $k_1 = 1$; **(a)** $\Omega = 0$, $\beta = 0$, **(b)** $\Omega = 0$, $\beta = 0.05$

In Fig. 5 cross-sections of the surface (44) of Fig. 4(b), known as the *Viaduct* [42], is shown in the (μ_1, μ_2) - plane for different values of the stiffness parameter κ. At $\kappa = 0$ the origin is inside the flutter domain while the stability region is bounded by a hyperbolic curve and belongs to the first quadrant of the plane. With the increase in κ the stability domain tends closer to the origin until at $\kappa = 2\beta$ it touches the origin, which is a singular point of the stability boundary. At this value of the stiffness parameter κ the origin corresponds to the double pure imaginary eigenvalue and the stability boundary has a cusp singularity at the origin [19-21, 61]. With the further increase in κ the zero angle at the cusp opens up and the stability boundary in the (μ_1, μ_2) - plane has a singularity corresponding to intersection of two curves at the origin. This is a typical evolution of the cross-sections of the stability domain of a circulatory system with dissipation [13, 15, 19-21, 61].

We see that stiffness modification that violates the symmetry of the system ($\kappa := k_2 - k_1 \neq 0$) enlarges the stability domain that extends to the origin in (μ_1, μ_2)-plane for sufficiently large κ. For such values of κ stabilization can be achieved even by infinitesimal amounts of damping for correctly chosen ratio of the damping coefficients.
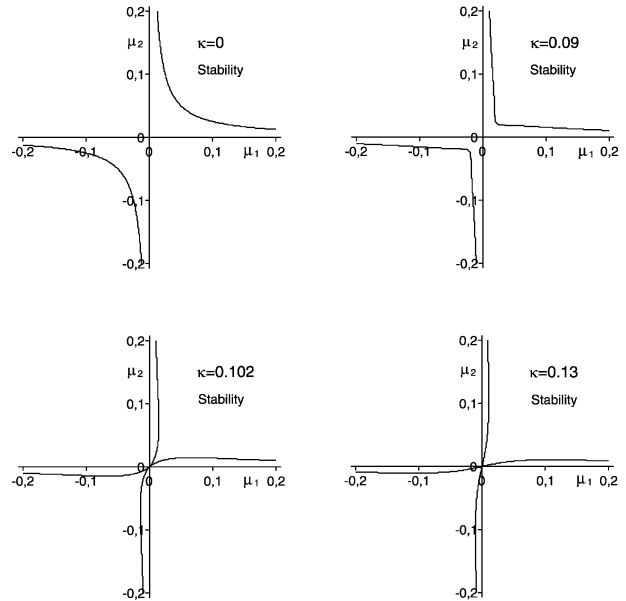

Fig. 5: Approximation to the asymptotic stability domain in the plane of the damping coefficients for various values of the stiffness parameter κ **and fixed** $\Omega = 0$ **and** $\beta = 0.05$

In the presence of all types of forces - gyroscopic, non-conservative positional and damping - the deviation of the stability boundary from the dihedral angle of Fig. 4(a) takes the most dramatical form, Fig. 6(a). Qualitatively, the singular surface, part of which bounds the stability domain, has again the viaduct [42, 55, 67] form. Non-conservative forces produce an instability window that is distorted by the gyroscopic ones, Fig. 6(a). As a consequence, the critical surface has self-intersections not along the κ - axis as it was for

$\Omega = 0$, but along the hyperbolic curves (36) that lie in the plane $\mu_1 + \mu_2 = 0$.

It is remarkable that on the curves all the eigenvalues of the non-conservative gyroscopic system with dissipative and circulatory forces are pure imaginary, see Fig. 6. Almost everywhere on the curves of self-intersection the eigenvalues are simple except for the points with the coordinates in the (μ_1, μ_2, κ)-space

$$(2\Omega m, -2\Omega m, 2\beta), \ (-2\Omega m, 2\Omega m, -2\beta), \quad (48)$$

where the pure imaginary eigenvalues are double and have a Jordan block, see Fig. 6.
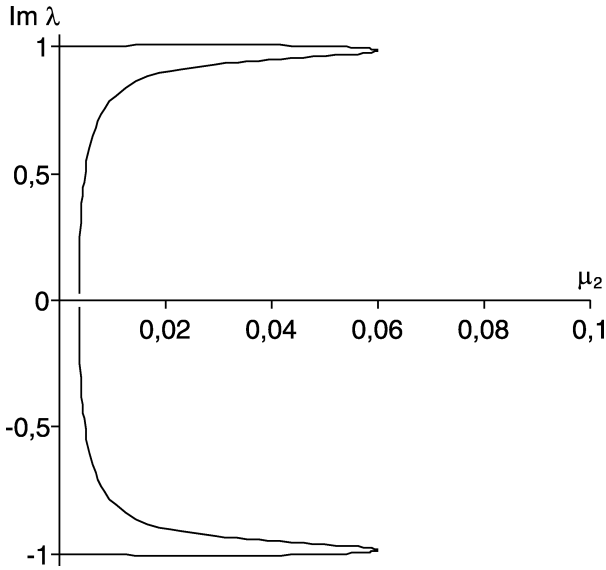

Fig. 6: Pure imaginary roots of the characteristic Eqn. (35) when parameters vary along the curve (36) for $m = 1$, $k_1 = 1$, $\Omega = 0.03$, **and** $\beta = 0.03$

Eqn. (41) gives an approximation to the exact double eigenvalue (38) up to the terms of first order with respect to the perturbation parameters

$$\lambda_{\pm} = i\sqrt{\frac{k_1}{m}} \pm i\frac{\beta}{2\sqrt{k_1 m}}. \quad (49)$$

The shape of the stability boundary shown in Fig. 7(a) is a fundamental and new phenomenon in comparison with the well-known stability domains of near-Hamiltonian or near-reversible systems such as that of the Ziegler pendulum [13-15, 19-21, 23, 24], where the marginally stable system with all its eigenvalues being pure imaginary corresponds to zero dissipation.

The consequences of such an unusual property of the stability boundary of system (33) are clearly seen in Fig. 8 where the cross-sections of the surface shown in Fig. 7(a) are plotted. For $\kappa = 0$ stability domain shown in Fig. 8 does not contain the origin, in accordance with the Bottema-Lakhadanov's theorem that states that a gyroscopic system with circulatory forces generically is unstable without dissipation [23, 51]. This theorem governs the evolution of the stability domain with the stiffness modification.

Indeed, the violation of the symmetry of the stiffness distribution that corresponds to the increase in

the parameter κ leads to the deformation of the stability boundary and its meeting with the other branch of the cross-section of the critical surface (44) outside the origin in the (μ_1, μ_2) - plane. At $\kappa = 2\beta$ stability domain has a cusp singularity at the point $(2\Omega m, -2\Omega m)$ that transforms into the simple intersection point that drifts to the origin with the further increase in κ, Fig. 8.
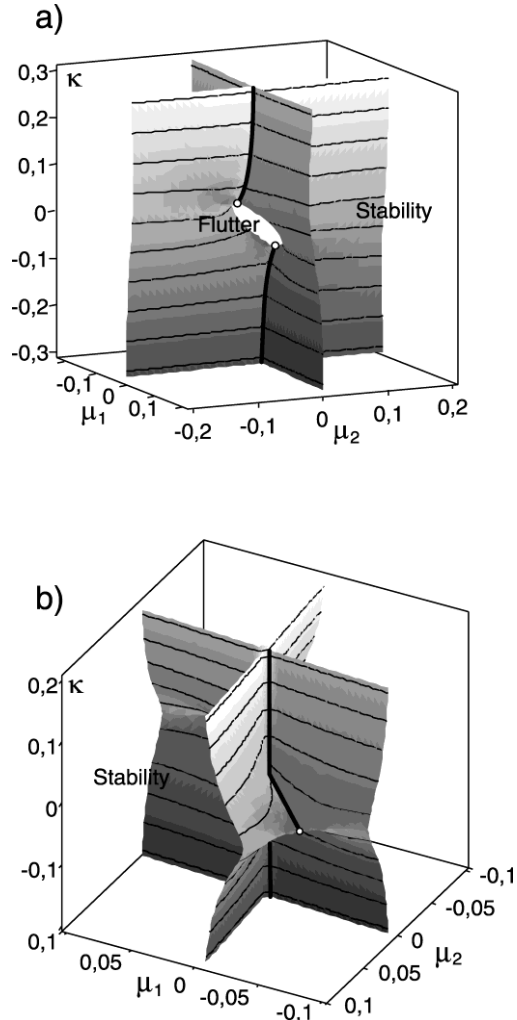

Fig. 7: Approximation to the asymptotic stability domain in the (μ_1, μ_2, κ) **- space for** $m = 1$, $k_1 = 1$; **(a)** $\Omega = 0.03, \beta = 0.03$, **(b)** $\Omega = 0.03$, $\beta = 0$

Fig. 8 shows that when the gyroscopic and non-conservative forces are simultaneously present, the origin in the (μ_1, μ_2) - plane is always unstable, whatever the value of stiffness modification parameter κ is. This happens because the non-conservative positional forces create a region of instability around the origin in the (μ_1, μ_2, κ) - space. This means that even when the frequencies of the stiffness matrix P are well-separated, one cannot stabilize the non-conservative gyroscopic system by arbitrarily small amount of damping with positive definite matrix of dissipative forces. There exist lower bounds on the values of the damping coefficients, the excess of which yields stabilization. Due to the non-symmetry of the stability domain the stabilizing distribution of damping is non-trivial.

It is remarkable that all the complicated transformations of the stability domain in the (μ_1, μ_2) - plane due to stiffness modification can easily be understood when we know the form of the three-dimensional stability domain in the (μ_1, μ_2, κ) - space. The viaduct is a universal relatively simple singular surface that naturally appears both in the gyroscopic (Fig. 7(a)) and non-gyroscopic (Fig. 4(b)) case in the presence of non-conservative positional forces. It should be noted, however, that in the limit $\beta \to 0$ at $\Omega \neq 0$ the viaduct critical surface transforms into one without a central hole, Fig. 7(b). The hyperbolas (36) degenerate into two straight lines that intersect at the origin, where there appears a singularity known as the *intersection of self-intersections* [73].
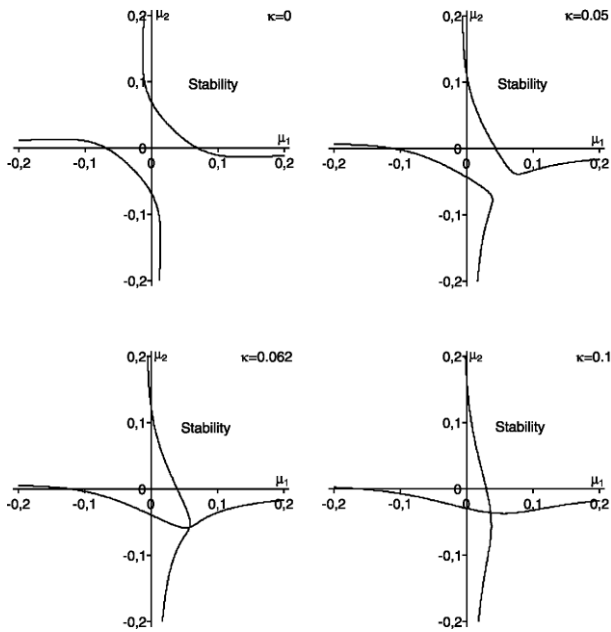

Fig. 8: Approximation to the asymptotic stability domain in the plane of damping coefficients for different values of the stiffness parameter and fixed $\Omega = 0.03$ **and** $\beta = 0.03$

It is seen that in the (μ_1, μ_2, κ) - space in the absence of non-conservative positional forces, i.e. for $\beta = 0$, the critical surface is diffeomorphic to the classical singular surface known as the Plücker conoid of index $n = 1$ [73].

In Fig. 9 we plot the cross sections of the critical surface in the plane of the damping parameters. In the case of the conservative gyroscopic system the origin is always on the stability boundary. The marginally stable gyroscopic system with the positive definite matrix of potential forces is stabilized by the arbitrary dissipative forces with the full dissipation in accordance with the Kelvin-Tait-Chetaev theorem [62]. It seen, however, that for a symmetric stiffness distribution the stability domain is wider than for a non-symmetric one.

We conclude that the double semi-simple pure imaginary eigenvalue corresponding to the undamped shaft without non-conservative positional forces is indeed a source of instability in the subcritical speed range. The most destabilizing influence on its splitting is

given by the circulatory forces. This destabilization is perfectly visualized in the (μ_1, μ_2, κ) -space of the damping and stiffness modification parameters, where the typical stability boundary is a part of the viaduct singular surface with the opening around the origin. This opening prevents stabilization of the non-conservative gyroscopic system by small amounts of damping.
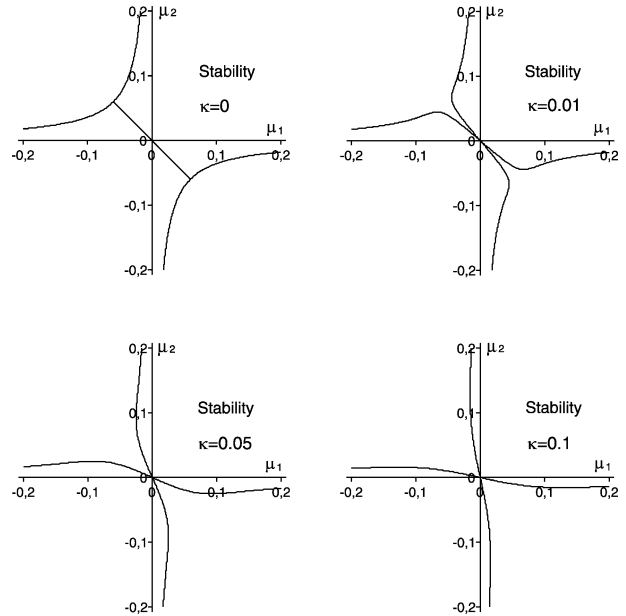

Fig. 9: Approximation to the asymptotic stability domain in the plane of damping coefficients for different values of the stiffness parameter and fixed $\Omega = 0.03$ **and** $\beta = 0$

For stabilization a considerably large damping coefficients are required taken in the right proportion that is influenced by the Whitney umbrella singularity at the exceptional points of the critical surface. Understanding the form of the stability boundary and its singularities for the perturbed 1:1 resonance on the example of the rotating shaft clarifies the prospective and limitations of optimisation of rotating continua in frictional contact, such as brakes, by means of stiffness modification. On the other hand, it shows how stability characteristics of rotating continua in frictional contact could be influenced by wear that changes the stiffness distribution of, for example, brake pads.

5. Conclusions

We investigated stability of a non-conservative gyroscopic system that arises in the modelling of rotating continua in frictional contact. Applying the perturbation theory of multiple eigenvalues to the doublets in the subcritical speed range we found explicit formulas that describe unfolding of the doublets due to stiffness modification and perturbation by dissipative, circulatory and gyroscopic forces.

The perturbation theory reproduces the exact expression for the marginal stability domain in a model of a brake disc in frictional contact. The instability domain of this model has conical singularities that are associated with the doublets in the spectrum of the symmetric problem and are typical in circulatory systems. The conical instability tongues are oriented in

the 'contact span angle – friction coefficient' - plane in accordance with the classical Merkin theorem that states destabilization of a potential system with the coincident eigenfrequencies by the non-conservative positional forces. The same singularity on the boundary of the domain of marginal stability was found in the model of a rotating shaft.

On the example of the rotating shaft we established that the asymptotic stability domain in the space of two damping parameters and the stiffness parameter has a complicated boundary with the self-intersections and Whitney umbrella singularities. On the singular set all the eigenvalues of the gyroscopic system are pure imaginary despite the presence of damping and non-conservative positional forces. This discovery clarifies difficulties with the stabilization of non-conservative gyroscopic systems and is useful for the problems of structural optimisation of the elements of brakes as well as for the studies of wear and its influence on stability of rotating continua in frictional contact.

ACKNOWLEDGEMENT:

REFERENCES:

[1] C. Cantoni, R. Cesarini, G. Mastinu, G. Rocca and R. Sicigliano. 2009. Brake comfort - a review, *Vehicle System Dynamics*, 47(8), 901-947. doi:10.1080/00423110903100432

[2] N.M. Kinkaid, O.M O'Reilly and P. Papadopoulos. 2003 Automotive disc brake squeal, *J. Sound Vibration,* 267, 105-166. doi:10.1016/S0022-460X(02)01573-0

[3] N. Hoffmann and L. Gaul. 2003. Effects of damping on mode-coupling instability in friction-induced oscillations. *Z. angew. Math. Mech.*, 83, 524-534. doi:10.1002/zamm.200310022

[4] J. Kang, C.M. Krousgrill and F. Sadeghi. 2008. Dynamic instability of a thin circular plate with friction interface and its application to disc brake squeal, *J. Sound Vibration*, 316(1-5), 164–179.

[5] J. Kang, C.M. Krousgrill and F. Sadeghi. 2009. Comprehensive stability analysis of disc brake vibrations including gyroscopic, negative friction slope and mode-coupling mechanisms, *J. Sound Vibration,* 324 387-407. doi:10.1016/j.jsv.2009.01.050

[6] J. Kang, C.M. Krousgrill and F. Sadeghi. 2009. Analytical formulation of mode-coupling instability in disc–pad coupled system, *Int. J. Mech. Sci.,* 51, 52-63. doi:10.1016/j.ijmecsci.2008.11.002

[7] U. von Wagner, D. Hochlenert and P. Hagedorn. 2007. Minimal models for disk brake squeal, *J. Sound Vibration*, 302, 2007, 527-539. doi:10.1016/j.jsv.2006.11.023

[8] O.N. Kirillov. 2008. Subcritical flutter in the acoustics of friction, *Proc. R. Soc. Lond., A*, 464(2097) 2321–2339. doi:10.1098/rspa.2008.0021

[9] O.N. Kirillov. 2010. Eigenvalue bifurcation in multiparameter families of non-self-adjoint operator matrices, *Z. Angew. Math. Phys.,* 61(2), 221-234. doi:10.1007/s00033-009-0032-0

[10] R. Meifal and O. Masaaki. 2007. Effect of surface topography on mode-coupling model of dry contact sliding systems, *J. Sound Vibration,* 308, 721–734. doi:10.1016/j.jsv.2007.03.046

[11] J.E. Mottershead and S.N. Chan. 1995. Flutter instability of circular discs with frictional follower loads, *Trans. ASME J. Vib. Acoust.,* 177, 161-163. doi:10.1115/1.2873860

[12] M.R. North. 1976. Disc brake squeal, in: Braking of Road Vehicles, Automobile Division of the Inst. of Mechanical Engineers*, Mechanical Engineers Publications Limited*, London, England, 169-176.

[13] J.J. Sinou and L. Jezequel. 2007. Mode coupling instability in friction-induced vibrations and its dependency on system parameters including damping, *Eur. J. Mech. A.,* 26, 106-122. doi:10.1016/j.euromechsol.2006.03.002

[14] G.S. Korspeter, O.N. Kirillov and P. Hagedorn. 2008. Modeling and stability analysis of an axially moving beam with frictional contact, *Trans. ASME, J. Appl. Mech.,* 75(3), 031001. doi:10.1115/1.2755166

[15] O.N. Kirillov and F. Verhulst. 2010. Paradoxes of dissipation-induced destabilization or who opened Whitney's umbrella? *Z. Angew. Math. Mech.,* 90, 462-488. doi:10.1002/zamm.200900315

[16] A.R. Abu Bakar, H. Ouyang. 2006. Complex eigenvalue analysis and dynamic transient analysis in predicting disc brake squeal, *Int. J. Vehicle Noise and Vibration*, 2, 143-155. doi:10.1504/IJVNV.2006.011051

[17] M. L. Chargin, L. W. Dunne and D. N. Herting. 1997. Nonlinear dynamics of brake squeal, *Finite Elements in Analysis and Design,* 28, 69-82. doi:10.1016/S0168-874X(97)81963-4

[18] O.N. Kirillov. 2000. Analysis of stability boundaries and optimization of circulatory systems, *PhD Thesis, M.V. Lomonosov Moscow State University*, Moscow, Russia.

[19] O.N. Kirillov. 2004. Destabilization paradox, *Dokl. Phys.,* 49(4), 239-245. doi:10.1134/1.1753620

[20] O.N. Kirillov. 2005. A theory of the destabilization paradox in non-conservative systems, *Acta Mech.,* 174, 145-166. doi:10.1007/s00707-004-0194-y

[21] O.N. Kirillov. 2007. Destabilization paradox due to breaking the Hamiltonian and reversible symmetry, *Int. J. Non-Linear Mech.,* 42(1), 71-87. doi:10.1016/j.ijnonlinmec.2006.09.003

[22] W. Kliem and C. Pommer. 2008. Indefinite damping in mechanical systems and gyroscopic stabilization, *Z. angew. Math. Phys.,* 60, 785-795. doi:10.1007/s00033-007-7072-0

[23] O. Bottema. 1955. On the stability of the equilibrium of a linear mechanical system, *Z. angew. Math. Phys.,* 6, 97-104. doi:10.1007/BF01607296

[24] O. Bottema. 1956. The Routh-Hurwitz condition for the biquadratic equation, *Indag. Math.*, 18, 403-406.

[25] V.I. Arnold. 1983. *Geometrical Methods in the Theory of Ordinary Differential Equations*, New York: Springer-Verlag.

[26] J.D. Fieldhouse, N. Ashraf and C. Talbot. 2008. *The measurement and analysis of the disc/pad interface dynamic centre of pressure and its influence on brake noise*, SP-2188, Brake Tech., SAE Paper 2008-01-0826.

[27] F. Massi, Y. Berthier and L. Baillet. 2008. Contact surface topography and system dynamics of brake squeal, *Wear*, 265, 1784-1792.

[28] A.R. Abu Bakar, H. Ouyang. 2008. Wear prediction of friction material and brake squeal using the finite element method, *Wear*, 264, 1069-1076.

[29] H.J. Soh and J.-H. Yoo. 2010. Optimal shape design of a brake calliper for squeal noise reduction considering system instability. *Proc. IMechE Part D: J. Automobile Eng.,* 224, 909-925. doi:10.1243/09544070JAUTO1385

[30] G. Spelsberg-Korspeter, D. Hochlenert, O.N. Kirillov and P. Hagedorn. 2009. In- and out-of-plane vibrations of a rotating plate with frictional contact: investigations on squeal phenomena. *Trans. ASME J. Appl. Mech.,* 76, 041006. doi:10.1115/1.3112734

[31] G. Genta. 2007. Dynamics of Rotating Systems, Springer, New York.

[32] A. Muszynska. 1986. Whirl and whip – rotor bearing stability problems, *J. Sound Vibration,* 110(3), 443-462. doi:10.1016/S0022-460X(86)80146-8

[33] A. Muszynska. 1988. Stability of whirl and whip in rotor/bearing systems, *J. Sound Vibration,* 127(1), 49-64. doi:10.1016/0022-460X(88)90349-5

[34] K. Ono, J.-S. Chen and D.B. Bogy. 1991. Stability analysis for the head-disk interface in a flexible disk drive. *Trans. ASME J. Appl. Mech.,* 58, 1005-1014. doi:10.1115/1.2897675

[35] J.-S. Chen and D.B. Bogy. 1992. Mathematical structure of modal interactions in a spinning disk-stationary load system, *Trans. ASME J. Appl. Mech.,* 59, 390-397. doi:10.1115/1.2899532

[36] S.G. Hutton, S. Chonan and B.F. Lehmann. 1987. Dynamic response of a guided circular saw, *J. Sound Vibration,* 112, 527-539. doi:10.1016/S0022-460X(87)80116-5

[37] J.E. Mottershead. 1998. Vibration- and friction-induced instabilities in discs, *Shock and Vibr., Digest,* 30, 14-31. doi:10.1177/058310249803000103

[38] W. Nagata and N.S. Namachchivaya. 1998. Bifurcations in gyroscopic systems with an application to rotating shafts, *Proc. R. Soc. Lond., A,* 454, 543-585. doi:10.1098/rspa.1998.0174

[39] T.H. Young and C.Y. Lin. 2006. Stability of a spinning disk under a stationary oscillating unit. *J. Sound Vibration,* 298, 307-318. doi:10.1016/j.jsv.2006.05.024

[40] W.D. Iwan and K.J. Stahl. 1973. The response of an elastic disc with a moving mass system, *Trans. ASME J. Appl. Mech.,* 40, 445-451. doi:10.1115/1.3423004

[41] N.C. Perkins and C.D. Mote. 1986. Comments on curve veering in eigenvalue problems, *J. Sound Vibration,* 106, 451-463. doi:10.1016/0022-460X(86)90191-4

[42] O.N. Kirillov. 2009. Campbell diagrams of weakly anisotropic flexible rotors, *Proc. R. Soc., A,* 465, 2703-2723. doi:10.1098/rspa.2009.0055

[43] R.S. MacKay. 1986. Stability of equilibria of Hamiltonian systems. In *Nonlinear phenomena and chaos* (ed. S. Sarkar), pp. 254-270. Bristol, UK: Adam Hilger.

[44] G.S. Schajer. 1984.. The vibration of a rotating circular string subject to a fixed end restraint, *J. Sound Vibration,* 92, 11-19. doi:10.1016/0022-460X(84)90369-9

[45] Y. Xion and S. Hutton. 1994. Vibration and stability analysis of a multy-guided rotating string, *J. Sound Vibration,* 169(5), 669-683. doi:10.1006/jsvi.1994.1040

[46] L. Yang and S. Hutton. 1995. Interactions between an idealized rotating string and stationary constraints, *J. Sound Vibration*, 185, 139-154. doi:10.1006/jsvi.1994.0368

[47] J. Tian and S. Hutton. 1999. On the mechanisms of vibrational instability in a constrained rotating string. *J. Sound Vibration,* 225, 111-126. doi:10.1006/jsvi.1999.2237

[48] S.-P. Cheng and N.C. Perkins. 1991. The vibration and stability of a friction-guided, translating string, *J. Sound Vibration,* 144(2), 281-292. doi:10.1016/0022-460X(91)90749-A

[49] H. Ouyang and J.E. Mottershead. 2001. Unstable travelling waves in the friction-induced vibration of discs. *J. Sound Vibration,* 248, 768-779. doi:10.1006/jsvi.2001.3720

[50] J.E. Mottershead, H. Ouyang, M.P. Cartmell and M.I. Friswell. 1997. Parametric resonances in an annular disc, with a rotating system of distributed mass and elasticity; and the effects of friction and damping, *Proc. R. Soc. A.,* 453, 1-19. doi:10.1098/rspa.1997.0001

[51] V.M. Lakhadanov. 1975. On stabilization of potential systems, *Prikl. Mat. Mekh.*, 39, 53-58.

[52] J.D. Fieldhouse, W.P. Steel, C.J. Talbot and M.A. Siddiqui. 2004. Rotor asymmetry used to reduce disc brake noise, Brake Colloquium and Exhibition, October, Anaheim, CA, USA, *SAE Paper* 2004-01-2797.

[53] C.L. Penninger and R.A. Swift. 2004. Disc brake lining shape optimization by multibody dynamic analysis, SP-1866, ABS/TCS, Brake Tech.& Foundation Brake NVH, and Tire and Wheel Tech., *SAE Paper* 2004-01-0725.

[54] C.H. Riedel and C.A. Tan. 1998. Dynamic characteristics and mode localization of elastically constrained axially moving strings and beams, *J. Sound Vibration*, 104(2), 344-362.

[55] O.N. Kirillov. 2009. Perspectives and obstacles for optimisation of brake pads with respect to stability criteria, *Int. J. Vehicle Design*, 51(1/2) 143-167. doi:10.1504/IJVD.2009.027119

[56] O.N. Kirillov and A.P. Seyranian. 2002. Solution to the Herrmann-Smith problem, *Dokl. Phys.,* 47(10) 767-771. doi:10.1134/1.1519327

[57] A. Struthers and G. Jayaraman. 2010. Elastic stability of columns on partial elastic foundations under subtangential loading, *J. Sound Vibration*, 329, 3856-3865. doi:10.1016/j.jsv.2010.03.004

[58] T.M. Atanackovic, B.B. Jakovljevic and M.R. Petkovic. 2010. On the optimal shape of a column with partial elastic foundation, *Eur. J. Mech. A/Sols*, 29, 283-289.

[59] R. Krechetnikov and J.E. Marsden. 2006. On destabilizing effects of two fundamental nonconservative forces. *Physica D*, 214, 25-32. doi:10.1016/j.physd.2005.12.003

[60] D.R. Merkin. 1997. Introduction to the Theory of Stability, *Springer*, Berlin.

[61] R.H. Plaut. 1971. A new destabilization phenomenon in nonconservative systems, *Z. Angew. Math. Mech.,* 51(4), 319-321. doi:10.1002/zamm.19710510414

[62] E.E. Zajac. 1964. The Kelvin–Tait–Chetaev theorem and extensions, *J. Aeronaut Sci.*, 11(2) 46-49.

[63] L.E.J. Brouwer. 1918. Beweging van een materieel punt op den bodem eener draaiende vaas onder den invloed der zwaartekracht}, *N. Arch. v. Wisk.,* 2e reeks, 12, 407-419. (The motion of a particle on the bottom of a rotating vessel under the influence of the gravitational force, Collected works, Vol. II, 665-686, Amsterdam 1975).

[64] R.C. Shieh and E.F. Masur. 1968. Some general principles of dynamic instability of solid bodies. Z. Angew. Math. Phys., 19, 927-941. doi:10.1007/BF01602273

[65] O. Bottema. 1976. Stability of equilibrium of a heavy particle on a rotating surface, *Z. angew. Math. Phys.,* 27, 663-669. doi:10.1007/BF01591177

[66] R.I. Thompson, T.J. Harmon, and M.G. Ball. 2002. The rotating-saddle trap: a mechanical analogy to RF-electric quadrupole ion trapping? *Can. J. Phys.,* 80, 1433-1448. doi:10.1139/p02-110

[67] O.N. Kirillov, A.A. Mailybaev and A.P. Seyranian. 2005. Unfolding of eigenvalue surfaces near a diabolic point due to a complex perturbation. *J. Phys. A: Math. Gen.,* 38, 5531-5546. doi:10.1088/0305-4470/38/24/007

[68] R. Hryniv and P. Lancaster. 2001. Stabilization of gyroscopic systems. *Z. Angew. Math. Mech.,* 81, 675-681. doi:10.1002/1521-4001(200110)81:10<675::AID-ZAMM675>3.0.CO;2-R

[69] T. Butlin and J. Woodhouse. 2009. Friction-induced vibration: Should low-order models be believed? *J. Sound Vibration,* 328, 92-108. doi:10.1016/j.jsv.2009.08.001

[70] V.V. Bolotin. 1963. Non-conservative Problems of the Theory of Elastic Stability, Fizmatgiz (in Russian), Moscow, Pergamon, Oxford.

[71] A.M. Gasparini, A.V. Saetta and R.V. Vitaliani. 1995. On the stability and instability regions of non-conservative continuous system under partially follower forces, *Comput. Methods Appl. Mech. Engrg.,* 124, 63-78. doi:10.1016/0045-7825(94)00756-D

[72] M.A. Langthjem and Y. Sugiyama. 2000. Dynamic stability of columns subjected to follower loads: a survey, *J. Sound Vibration,* 238, 809-851. doi:10.1006/jsvi.2000.3137

[73] I. Hoveijn and O.N. Kirillov. 2010. Singularities on the boundary of the stability domain near 1:1 resonance, *J. Differ. Equ.,* 248(10), 2585-2607. doi:10.1016/j.jde.2009.12.004